Molecular Therapy
Methods & Clinical Development
Original Article

Hair Cell Transduction Efficiency of Single- and Dual-AAV Serotypes in Adult Murine Cochleae

Ryotaro Omichi,[1,2,8] Hidekane Yoshimura,[1,3,8] Seiji B. Shibata,[1,4] Luk H. Vandenberghe,[5,6] and Richard J.H. Smith[1,4,7]

[1]Molecular Otolaryngology and Renal Research Laboratories, Carver College of Medicine, University of Iowa, 285 Newton Road, 5270 CBRB, Iowa City, IA 52242, USA; [2]Department of Otolaryngology–Head and Neck Surgery, Okayama University Graduate School of Medicine, Dentistry and Pharmaceutical Sciences, 2-5-1 Shikata-Cho, Kita-Ku, Okayama 700-8558, Japan; [3]Department of Otorhinolaryngology, Shinshu University School of Medicine, Matsumoto, Nagano 390-8621, Japan; [4]Department of Otolaryngology–Head and Neck Surgery, Carver College of Medicine, University of Iowa, Iowa City, IA 52242, USA; [5]Grousbeck Gene Therapy Center, Ocular Genomics Institute, Schepens Eye Research Institute and Mass Eye and Ear, Boston, MA, USA; [6]The Broad Institute of Harvard and MIT, Cambridge, MA, USA; [7]Iowa Institute of Human Genetics, Carver College of Medicine, University of Iowa, Iowa City, IA 52242, USA

Gene delivery is a key component for the treatment of genetic hearing loss. To date, a myriad of adeno-associated virus (AAV) serotypes and surgical approaches have been employed to deliver transgenes to cochlear hair cells, but the efficacy of dual transduction remains unclear. Herein, we investigated cellular tropism of single injections of AAV serotype 1 (AAV1), AAV2, AAV8, AAV9, and Anc80L65, and quantitated dual-vector co-transduction rates following co-injection of AAV2 and AAV9 vectors in adult murine cochlea. We used the combined round window membrane and canal fenestration (RWM+CF) injection technique for vector delivery. Single AAV2 injections were most robust and transduced 96.7% ± 1.1% of inner hair cells (IHCs) and 83.9% ± 2.0% of outer hair cells (OHCs) throughout the cochlea without causing hearing impairment or hair cell loss. Dual AAV2 injection co-transduced 96.9% ± 1.7% of IHCs and 65.6% ± 8.95% of OHCs. Together, RWM+CF-injected single or dual AAV2 provides the highest auditory hair cell transduction efficiency of the AAV serotypes we studied. These findings broaden the application of cochlear gene therapy targeting hair cells.

INTRODUCTION

In monogenic diseases, gene therapy can be employed to correct or suppress a mutant gene, or to replace a wild-type gene, thereby achieving successful habilitation.[1] The delivery of the transgene to the relevant target tissue is a key component to successful gene therapy, with viral vectors commonly utilized for this purpose because their transduction properties are superior to non-viral vectors.[2] Among viral vectors, adeno-associated viruses (AAVs) have become increasingly popular as a gene delivery vector for virus-based gene therapies, with two AAV-based gene therapies currently approved by the US Food and Drug Administration: LUXTURNA (voretigene neparvovec-rzyl) for Leber's congenital amaurosis and ZOLGENSMA (onasemnogene abeparvovec-xioi) for spinal muscular atrophy.

The characteristics of broad cellular tropism, non-ototoxicity, and low immunogenicity have also attracted interest in utilizing AAVs for inner ear therapeutic applications.[3] Because approximately two-thirds of all genes implicated in non-syndromic sensorineural hearing loss are expressed in both inner hair cells (IHCs) and outer hair cells (OHCs),[4] gene delivery methods that target both cell types are necessary to restore full auditory sensitivity.[5] Currently, the cellular tropism of 12 naturally occurring serotypes of human AAVs and several other synthetic AAVs has been characterized.[1] Studies have defined the *in vivo* transduction properties of these AAV serotypes in neonatal and adult murine ear using various inoculation methods.[6–10] In aggregate, these studies have demonstrated that multiple factors, including age, vector serotype, promoter type, injection method, and viral titers, impact cellular tropism and transduction efficiency in the murine inner ear.[1] Importantly, several AAV serotypes, such as AAV 2/1 (AAV1), 2/2 (AAV2), 2/8 (AAV8), 2/9 (AAV9), and 2/Anc80L65 (Anc80), have been reported to transduce IHCs consistently, although gene transfer to the OHCs has been variable.[5]

Substantial efforts have also focused on developing an intracochlear delivery method that permits broad and robust inner ear transduction. We recently described one such method that combines round window membrane injection and canal fenestration (RWM+CF).[4] This approach facilitates circulation of the vector throughout the cochlea by creating a ventilation hole in the posterior semi-circular canal. The result is broad distribution of the viral suspension in the perilymph, thereby enhancing overall transduction. To date, however,

Received 4 February 2020; accepted 7 May 2020;
https://doi.org/10.1016/j.omtm.2020.05.007.

[8]These authors contributed equally to this work.

Correspondence: Richard J.H. Smith, MD, Molecular Otolaryngology and Renal Research Laboratories, Carver College of Medicine, University of Iowa, 285 Newton Road, 5270 CBRB, Iowa City, IA 52242, USA.
E-mail: richard-smith@uiowa.edu

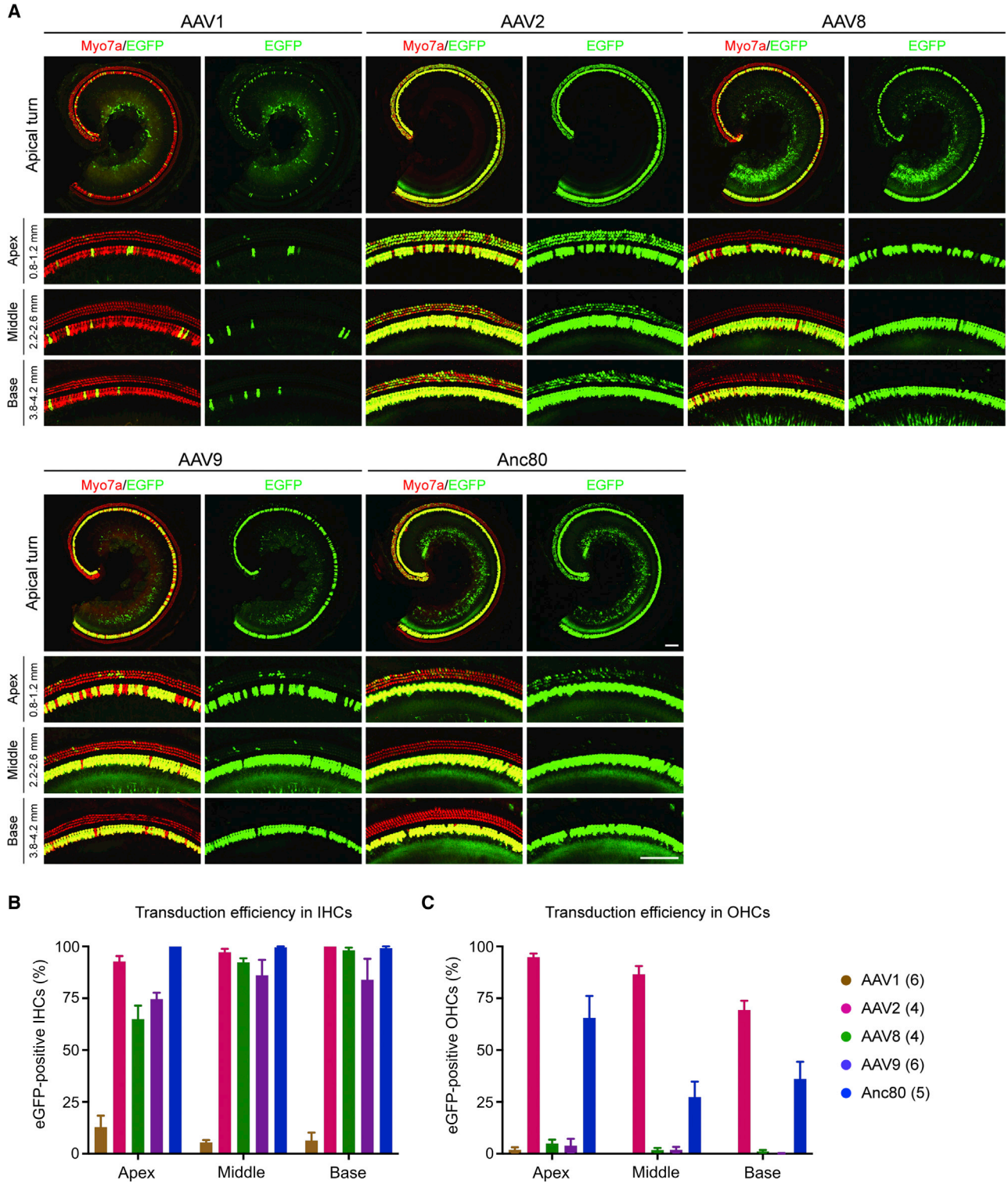

Figure 1. Transduction of IHCs and OHCs in Adult Mice Is Most Efficient with AAV2 Delivered Using the RWM+CF Injection Approach

(A) Cochleae harvested 2 weeks after administrating five AAV serotypes through RWM+CF in 4-week-old C3H/FeJ mice. Representative low-magnification images of whole-mount apical turns and high-magnification images of regions along cochlea duct 0.8–1.2 mm (apex), 2.2–2.6 mm (middle), and 3.8–4.2 mm (base) from the apical tip.

(legend continued on next page)

the inner ear transduction profile of hair cell-specific AAV subtypes has not been fully explored with RWM+CF injection.[1]

AAVs have a small viral loading capacity: no more than 5.0 kb can be inserted.[11,12] This limitation is significant because the coding sequence of many causative genes exceeds the loading capacity of a single AAV.[13,14] To circumvent this problem, researchers have adapted the dual-vector approach to enable delivery of larger transgenes.[13,14] This method utilizes the intrinsic property of AAV to undergo concatamerization when separate vectors co-transduce a single cell. Importantly, efficient dual-vector co-transduction in the target tissue is essential to achieve successful gene expression levels of these large coding sequences. Although the co-transduction efficiency of dual vectors in retina and neurons has been investigated, the dual-vector co-transduction rate in the inner ear has not been analyzed in adult mice.[15]

To identify AAV serotypes that transduce both mature murine IHCs and OHCs, we first selected five AAV serotypes, AAV1, AAV2, AAV8, AAV9, and Anc80, to inject into the cochlea using the RWM+CF technique. All vectors carried a CMV-driven EGFP transgene and the woodchuck hepatitis post-transcriptional virus regulatory element (WPRE) cassette. Viral suspensions were equal at 3.75–3.80 $\times$ 10^{12} genome copy (GC)/mL, allowing fair comparison and assessment of the cellular tropism of each AAV serotype. We then assessed dual-vector co-transduction efficiency in the cochlea following RWM+CF co-injection of combinations of AAV2 or AAV9 vectors expressing either EGFP or mCherry fluorescent protein.

Herein, we demonstrate that a single AAV2 injection transduces 96.7% ± 1.1% of IHCs and 83.9 ± 2.0% of OHCs (mean ± standard error) in adult mice without causing hearing impairment or hair cell (HC) loss. Dual-vector co-transduction with AAV2-EGFP and AAV2-mCherry is comparable (IHC transduction, 96.9% ± 1.7%; OHC transduction, 65.6% ± 9.0%). Thus, both single- and dual-AAV2-mediated gene transfer delivered via the RWM+CF approach enable efficient and specific HC transduction in a mature mouse model. These findings expand the application of cochlear gene therapy targeting mechanosensory hair cells in the inner ear.

RESULTS

RWM+CF Injection with AAV2 Leads to High IHC and OHC Transduction in All Cochlear Turns

To investigate the transduction profile of five AAV serotypes, we injected the left ear in 4-week-old C3H/FeJ mice using the RWM+CF technique. Two weeks later, both ears were harvested and quantitated in whole-mount preparations. Quantification of IHC transduction showed nearly total GFP localization in IHCs in all turns of the cochlea with both AAV2 (apex 92.8% ± 5.1%, middle 97.2% ± 3.2%, base 100%; overall 96.7% ± 1.1%) and Anc80 (apex 100%, middle 99.5% ± 1.1%, base 99.2% ± 1.8%) (Figures 1A and 1B). AAV8 and AAV9 also demonstrated robust transgene expression in IHCs throughout the cochlea duct (AAV8: apex 64.9% ± 13.0%, middle 92.3% ± 3.9%, base 98.1% ± 2.7%; AAV9: apex 64.9% ± 13.0%, middle 92.3% ± 3.9%, base 98.1% ± 2.7%, respectively), whereas AAV1 transduction of IHC was the least efficient among all serotypes (apex 12.8% ± 9.6%, middle 5.5% ± 2.0%, base 6.3% ± 6.8%). AAV2 demonstrated the highest OHC transduction with an apex-to-base gradient (apex 94.9% ± 3.5%, middle 86.5% ± 8.0%, base 69.4% ± 8.8%; overall 83.9% ± 2.0%). OHC transduction utilizing Anc80 was lower (apex 65.6% ± 23.6%, middle 27.4% ± 16.7%, base 36.1% ± 18.4%) (Figures 1A and 1C). GFP distribution in OHCs with AAV1, AAV8, and AAV9 was poor in all turns (<5%). These observations indicate that HC tropism is serotype specific, and that among five equally titrated AAV serotypes, AAV2 has the highest total IHC and OHC transduction rate.

AAV1, AAV2, AAV9, and Anc80 Do Not Change Auditory Thresholds or Cause Degeneration of Hair Cells

We investigated auditory function by measuring auditory brainstem response (ABR) thresholds 2 weeks after administration of each AAV vector to assess potential functional ototoxicity. Both ears were measured in all animals from each group, with the right ear serving as a control. In four serotypes of AAVs (AAV1, AAV2, AAV9, and Anc80), we observed no statistically significant differences in click and tone-burst ABRs across all frequencies between ears. However, injection of AAV8 led to an elevated click-evoked ABR threshold shift of 12 dB as compared with contralateral ears, whereas tone-burst ABRs remained comparable between ears (Figure 2). These findings suggest that the injection of AAV serotypes into the adult mouse cochlea does not alter auditory function, perhaps with the exception of AAV8. In daily monitoring of the postoperative health of the treated mice, we did observe transient circling behavior immediately after surgery that resolved within 24 h. No other behavioral side effects were noted (e.g., head tilting, weight loss, circling, or ear infection). To investigate potential cellular ototoxicity of each AAV serotype, we quantitated hair cell survival in RWM+CF-injected and non-injected ears in whole-mount preparations along the entire extent of the cochlear duct. Figure 3 indicates that IHC and OHC survival rates are comparable between injected and non-injected ears for all serotypes, with modest reductions for IHCs in the Anc80 condition and OHCs in the AAV8 condition.

Vestibular Organs Are Effectively Transduced following AAV8, AAV9, and Anc80 Injection

Quantitative assessment of whole-mount preparations of vestibular saccule epithelia revealed robust EGFP expression in vestibular HCs following AAV8, AAV9, and Anc80 injection (30.0% ± 13.1%,

Cochleae were stained with Myo7a (red) for labeling and imaged for native EGFP (green). Scale bar, 100 μm. (B and C) Quantitative comparison of IHC (B) and OHC (C) transduction efficiency assessed in 400-μm segments across different regions of the cochlea (apex, middle, and base) following the RWM+CF injection of various AAV serotypes. Data are represented as mean ± SEM.

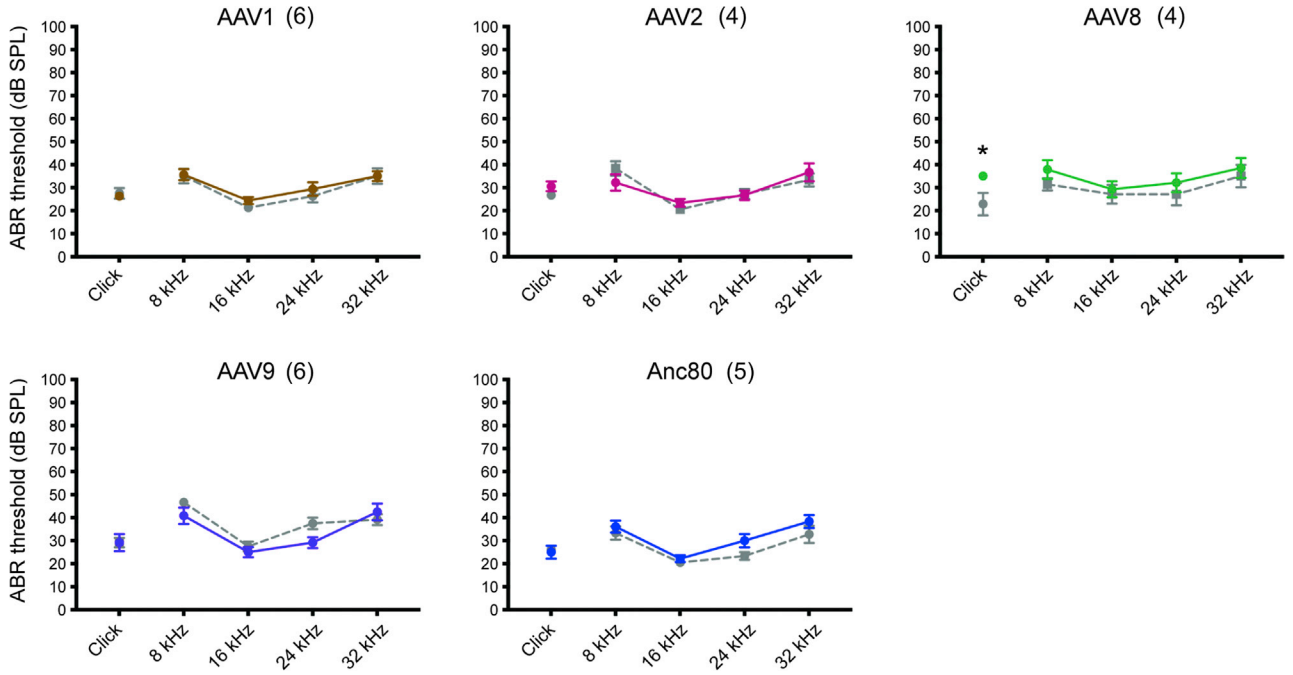

Figure 2. RWM+CF Injection Does Not Change ABR Thresholds in Adult Mice

Click and tone-burst ABRs show auditory thresholds in injected (solid lines) and non-injected (dashed lines) ears were comparable following delivery of AAV1, AAV2, AAV9, and Anc80. Data are represented as mean ± SEM. Statistical analysis by Student's t test. *p < 0.05.

18.9% ± 1.3%, and 29.1% ± 10.4%, respectively) (Figure 4). We noted a predilection for transduction of type II hair cells, which generally constitute cells with nuclei closer to the endolymphatic side of the epithelium as compared with type I hair cells (Figure 5), consistent with observations when Anc80 is delivered by canalostomy injection.[16] AAV2 did not demonstrate saccular HC transduction, which is contrary to cochlear HC results, suggesting that AAV2 tropism is cochlear hair cell specific. The AAV1 demonstrated GFP expression in the non-sensory tissue of the vestibule.

Partial Transduction of the Stria Vascularis, Spiral Ganglion Cells, Saccules, and Scarpa's Ganglion Cells Is Observed

To define the non-sensory transduction profile of AAVs within the organ of Corti (i.e., supporting cells [SCs], stria vascularis [SV], spiral ganglion cells, saccules, and Scarpa's ganglion cells), we analyzed cochlear and vestibular frozen cross sections in injected mice (Figure 5). EGFP transgene expression was detected in the SV in all AAV serotypes with the exception of AAV2. Vectors AAV8, AAV9, and Anc80 showed some degree of EGFP signal in spiral ganglion cells and Scarpa's ganglion cells. We did not detect EGFP expression in SCs of the organ of Corti, including pillar cells and interphalangeal cells.

Co-transduction with Dual AAV2 Demonstrates Comparable IHC and OHC Transduction Rates to Single AAV2

The following combinations of dual vectors were injected into the left ear in 4-week-old mice using the RWM+CF technique: AAV2-EGFP and AAV2-mCherry (hereafter noted as AAV2-2), AAV2-EGFP and AAV9-mCherry (AAV2-9), and AAV9-EGFP and AAV9-mCherry (AAV9-9). For each pair, we evaluated the co-transduction ratio; i.e., the ratio at which both vectors transduced the same cell. For comparison, we performed single-vector injection with AAV2-EGFP, AAV2-mCherry, AAV9-EGFP, and AAV9-mCherry.

With AAV2-2, we observed robust co-transduction of IHCs and OHCs (IHCs: apex 94.6% ± 4.7%, middle 98.1% ± 1.9%, base 98.1% ± 1.5%; OHCs: apex 93.0% ± 4.4%, middle 80.0% ± 9.6%, base 23.8% ± 12.9%) that was identical to that observed with either vector alone (AAV2-2 versus AAV2-EGFP in IHCs and OHCs: $p > 0.9999$ and $p > 0.9999$, respectively; AAV2-2 versus AAV2-mCherry in IHCs and OHCs: $p > 0.9999$ and $p > 0.9999$, respectively). IHC and OHC survival rates were comparable between injected and non-injected ears (Figure S1). Likewise, the co-transduction rates of AAV2-9 and transduction rate of AAV2-EGFP for IHCs were similar (AAV2-9 versus AAV2-EGFP in IHCs: apex $p > 0.9999$, middle $p > 0.9999$, base $p > 0.9999$). However, AAV2-9 co-transduction rates were significantly higher than AAV2-EGFP transduction rates for OHCs in the basal turn of the cochlea (AAV2-9 versus AAV2-EGFP in OHCs: apex $p = 0.0052$, middle $p = 0.0008$, base $p > 0.9999$) (Figure S2B). AAV2-9 and AAV9-mCherry transduction rates for IHCs and OHCs were comparable (AAV2-9 versus AAV9-mCherry in IHCs and OHCs: $p > 0.9999$ and $p > 0.9999$, respectively; AAV2-9 versus AAV9-mCherry in IHCs and OHCs, $p > 0.9999$ and $p > 0.9999$, respectively). Finally, with AAV9-9, transduction rates were significantly lower as compared with transduction

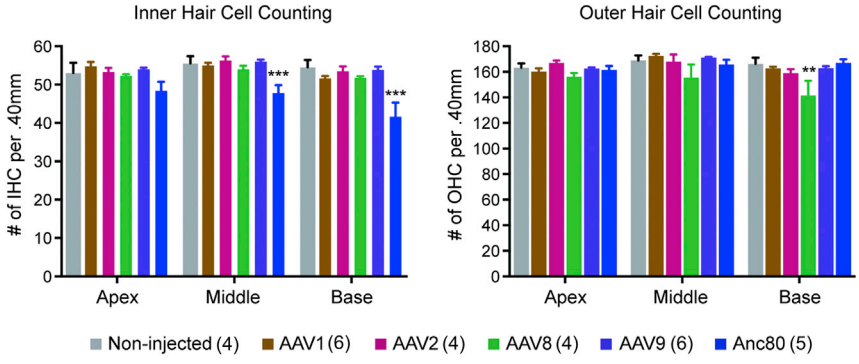

Figure 3. Quantitative Comparison of IHC and OHC Survival in Injected and Non-injected Ears Reveals that AAV8 and Anc80 Delivery Results in Hair Cell Loss

Hair cell counting in 400-μm segments across different regions of the cochlea (apex, middle, and base) as documented 2 weeks post-injection. Data are represented as mean ± SEM. Statisticalanalysis by one-way ANOVA. ***$p < 0.001$; **$p < 0.01$.

with AAV9-EGFP alone (AAV9-9 versus AAV9-EGFP: apex $p = 0.0026$, middle $p < 0.0001$, base $p = 0.0003$). Interestingly, IHC transduction of AAV9-mCherry in the base was higher with dual transduction than with single transduction ($p = 0.0152$) (Figure S2). All combinations had no hair cell loss (Figure S1).

DISCUSSION

The majority of genetic non-syndromic hearing loss is associated with genes expressed in the IHCs and/or OHCs, making the development of gene delivery vectors and injection methods that facilitate transduction of these cell types essential to gene therapy-based strategies to treat hearing loss.[4,5] We demonstrate that among five AAV serotypes tested (AAV1, AAV2, AAV8, AAV9, and Anc80) using a RWM+CF approach, transgene expression is most robust with AAV2 in both IHCs (97%) and OHCs (84%). Using dual vectors, we demonstrate that AAV2-2 co-transduction efficiency of hair cells is comparable with that observed with AAV2 alone. Auditory function and hair cell survival in injected versus non-injected ears are similar whether single- or dual-vector injections are performed, making AAV2 an excellent candidate vector for single and/or dual applications that require hair cell transduction.

Although AAV2 is the most commonly studied AAV serotype in the central nervous system (CNS), its utility in cochlear gene therapy studies has been limited, partially because of its poor tropism for hair cells in neonatal mouse cochlea.[6,7,10] For instance, when AAV1, AAV2, AAV8, and Anc80 are delivered to neonatal mouse cochlea through the RWM, EGFP transduction in IHCs and OHCs is poorest with AAV2.[7] In a recent study in the adult mouse cochlea in which AAV2 harboring GFP was delivered via canalostomy, however, near-total IHC transduction was observed, although OHC transduction was only partial (12.1% in the apex, 7.1% in the middle, and 1.6% in the base), despite using a 3-fold higher AAV2 titer than we used in this study (1×10^{13} versus 3.68×10^{12} GC/mL).[8] These differences in transduction efficiency and cell tropism suggest that animal age, strain, and method of delivery remain important determinants of outcome. Viral titer, viral purifying and processing differences, and the presence of WPRE also can impact GFP expression.[4,17] Interestingly, we found that AAV2 does not transduce vestibular hair cells despite robust transduction in cochlear hair cells, suggesting that AAV2 tropism is more specific than that of other AAVs.

New synthetic vectors such as Anc80 have emerged as an alternative to conventional AAV vectors, and transduce IHCs and OHCs with high efficiency when injected through either perilymph or endolymph in both neonatal and adult mice.[4,5,7,8,16,18] Consistent with previous reports, we demonstrated that Anc80 via RWM+CF injection in adult mice transduced virtually all IHCs.[8,16] Like others, we noted an apex-to-base gradient (apex 65.6% ± 23.6%, middle 27.4% ± 16.7%, base 36.1% ± 18.4%) in OHC transduction; however, our data demonstrated superior GFP transduction in the basal turn (36% versus 10%) when comparable viral titers are used,[8,16] suggesting that the RWM+CF technique may increase inner ear transduction efficiency. Irrespective of the AAV serotype we used, localization of EGFP signals in SCs was not achieved using the RWM+CF approach, a disappointing result that likely precludes the use of these AAVs for *GJB2*-focused gene therapy programs. Viral vectors such as AAV-inner ear, AAV2.7m8, bovine AAV, and adenovirus may be more suitable for selective SC transduction.[9,19–21]

It remains unclear why our results appear to diverge from those in prior studies, particularly the observed transduction rates of AAV1 and Anc80 for IHCs and OHCs, respectively, as compared with AAV2. By design, our study leverages a route of administration that differs from routes used in other studies assessing AAV transduction in the cochlea. Dose, titer, and transgene design can also lead to distinct differences in IHC and OHC transduction efficiency for a given viral vector. Lastly, not to be underestimated is the impact of genetic background. Our studies in C3H/FeJ mice may illustrate the dependency of route of administration, mouse strain, and age on the efficiency and tropism of AAV subtypes compared with prior studies in CBA/CaJ[16] and C57BL/6,[7,8] similar to observations with AAV-PHP.B in CNS targeting via systemic administration.[22,23]

In the vestibule, AAV8, AAV9, and Anc80 gave robust EGFP signals in the saccule, suggesting potential for these vectors with therapies designed to target both auditory and balance disorders. We also demonstrated that AAV9 and Anc80 provide limited transduction of spiral ganglion cells and Scarpa's ganglion cells, consistent with other studies injecting Anc80 via canalostomy.[16] To increase the transduction of these bipolar cell types, the development of a vector with neuron-specific tropism, using a neuron-specific promoter and/or increasing the viral titer, may be required.

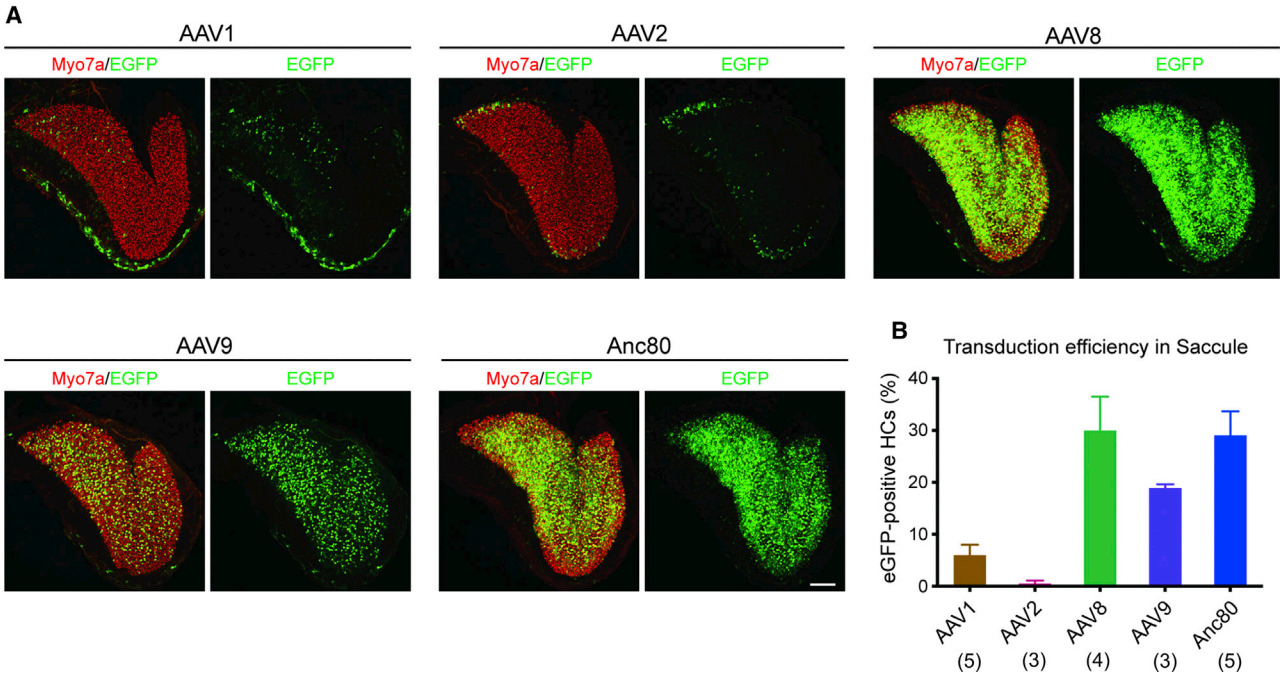

Figure 4. Saccular Hair Cells Are Transduced following the RWM+CF Injection with AAV8, AAV9, and Anc80

(A) Representative images of whole mounts of the saccule. Specimens were stained with Myo7a (red) for labeling and imaged for native EGFP (green). Scale bar, 100 μm. (B) Quantitative comparison of transduction efficiency after AAV injection as indicated. Data are represented as mean ± SEM.

The major disadvantage of AAV is its small packaging cargo (5.0 kb), because packaging efficiency sharply declines with sequences exceeding this limit.[11,12,24] To circumvent this limitation, a dual AAV vector system is needed to carry components of larger transgenes (>5 kb) that through various mechanisms are reconstituted. Choosing the right strategy can impact outcome. One approach employs homologous recombination: two halves of a large transgene in dual-AAV vectors share an overlapping region of cDNA and reconstitute to form a single large gene.[25] An alternative strategy is *trans*-splicing, whereby there is a splice donor site in one half of the gene and its splice acceptor site in the other half. After co-infection, *trans*-splicing occurs to reconstitute mRNA, which is translated into the complete protein.[26] This approach has been used successfully to express large genes in muscle and retina.[27,28] A hybrid AAV technique combines homologous recombination and *trans*-splicing. Alkaline phosphatase recombinogenic region (AP) or F1 phage recombinogenic region (AK) is included in each half of the divided gene to increase recombination between the dual AAVs.[29] A final approach uses inteins, which are self-catalytic protein splicing elements that self-excise to join the remaining protein portions together in a process termed protein splicing. Inteins have been used to demonstrate protein *trans*-splicing *in vitro* in mouse, pig, and human retinal organoids.[30]

Relevant to the ear are experiments by Al-Moyed et al.,[14] who inserted both halves of the 6-kb-long otoferlin cDNA in two distinct AAV6 vectors and included sequences to enable *trans*-splicing.[26] They co-injected into the cochlea of *Otof*$^{-/-}$ mice through the RWM at post-natal day 6 (P6) and P7. Akil et al.,[13] in comparison, engineered dual AAV2-quadY-F-CMV carrying half-coding sequences of *Otof* and injected *Otof*$^{-/-}$ mice via the RWM on P2, P17, or P30. Both groups demonstrated efficient *trans*-splicing in the context of a dual-vector approach for inner ear gene therapy. Importantly, while co-transduction is a minimum requirement, several other processes need to occur for OTOF protein expression to be realized, including concatemer formation to permit correct *trans*-splicing.[31] Our results establish the extent to which co-transduction may be rate limiting and demonstrate that for IHCs, AAV2 and AAV9 offer close to 100% transduction efficiency using a single-vector approach (Figure 1). A dual AAV2 system is equally robust (Figure 6). OHC co-transduction is less efficient, likely due to the fact that transduction with single vectors fails to reach 100%.

Importantly, our data indicate that co-transduction is *not* influenced by cooperation between the two vectors or by preferential selection of the hair cells (Figure 6; Figure S2), which is relevant because dual-vector transduction is believed to be inferior to single-vector transduction based on ocular and retinal studies.[29] For example, the retinal transduction efficiency of dual-AAV8 hybrid vectors was only 6% and 40% of the transduction rate with a single-AAV8 vector in mice and pigs.[29] We observed a similar trend with dual-AAV9-9/AAV9-EGFP expression, which was reduced while AAV9-mCherry was maintained, but for AAV2-2 and AAV2-9, co-transduction rates were similar to single-vector transduction rates. These results suggest

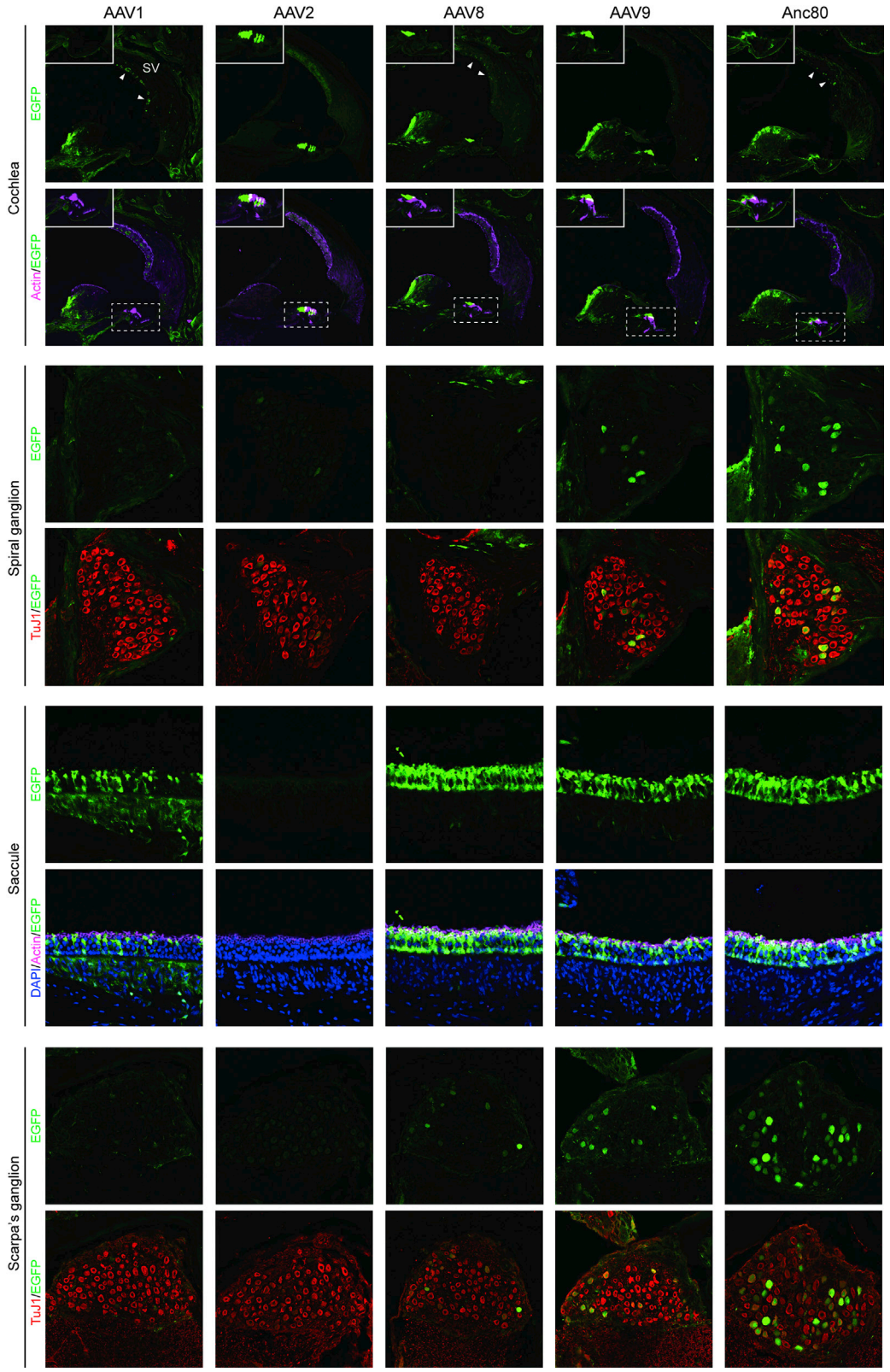

(legend on next page)

that specific combinations of dual vectors are likely to be important, an encouraging observation in view of retinal data that have led to substantial efforts to define compounds that enhance poor dual-AAV transduction efficiency in the eye.[29,31,32] One limitation of this study is that although we focused on co-transduction following dual-AAV delivery, we did not assess transgene expression levels following intermolecular concatamerization. Further studies are needed to address this question.

In conclusion, we have demonstrated excellent IHCs and OHCs transduction efficiency with AAV2 in adult mice following RWM+CF injection. Dual-vector co-transduction of AAV2-2 is equally robust and efficient. We therefore recommend AAV2 as a serotype to deliver small and large transgenes into IHCs and OHCs. Further studies are needed to evaluate the relevance of AAV2 in other species and human translation, as well the impact of the route of administration and mouse strain on these observations compared with those in prior studies. These results should help to guide studies using this vector and injection method to treat mature murine models of human deafness.

MATERIALS AND METHODS

Ethics Approvals

All experiments were approved by the University of Iowa Institutional Biosafety Committee (IBC; rDNA Committee; RDNA Approval Notice #100024) and the University of Iowa Institutional Animal Care and Use Committee (IACUC; Protocol #06061787), and were performed in accordance with the NIH *Guide for the Care and Use of Laboratory Animals*.

Virus Production

AAV1, AAV2, AAV8, AAV9, and Anc80 with a CMV-driven EGFP transgene and WPRE cassette were prepared by Gene Transfer Vector Core at the Mass Eye and Ear (https://www.vdb-lab.org/vector-core/). Droplet digital PCR (Bio-Rad, Hercules, CA, USA) was used for titration of all AAV preparations with primer sets for the transgene cassette according to the protocol published by Sanmiguel et al.[33] Viral titers were AAV1-EGFP at 3.75×10^{12} GC/mL, AAV2-EGFP at 3.68×10^{12} GC/mL, AAV8-EGFP at 4.94×10^{12} GC/mL, AAV9-EGFP at 1.20×10^{13} GC/mL, and Anc80-EGFP at 5.5×10^{12} GC/mL. For the dual-injection study, AAV2 and AAV9 carrying a mCherry-reporter gene and WPRE cassette were provided by the same laboratory. Viral titers were AAV2-mCherry at 2.15×10^{12} GC/mL and AAV9-mCherry at 2.48×10^{12} GC/mL. To compare transduction efficiency and safety at equal dose, we diluted AAV8, AAV9, and Anc80 with the final formulation buffer (FFB) to a concentration of $3.75–3.80 \times 10^{12}$ GC/mL for the single-vector injection. FFB is composed of 1X PBS + 35 mM NaCl + 0.001% PF-68. For the dual-vector experiment, vectors were mixed together with pipetting without FFB. The final concentrations were as follows: AAV2-EGFP at 1.84×10^{12} GC/mL, AAV2-mCherry at 1.07×10^{12} GC/mL, AAV9-EGFP at 1.2×10^{12} GC/mL, and AAV9-mCherry at 1.24×10^{12} GC/mL. Vector aliquots were stored at −80°C and thawed before use.

Animal Surgery

RWM+CF injection was carried out as described previously.[4] C3H/FeJ mice at 4 weeks of age were anesthetized with an intraperitoneal injection of ketamine (100 mg/kg) and xylazine (10 mg/kg). Body temperature was maintained with a heating pad during the surgical procedure. The left post-auricular region was shaved and cleaned. A post-auricular incision was made to access the temporal bone. The facial nerve was identified deep along the wall of the external auditory canal. After exposing the facial nerve and the sternocleidomastoid muscle, a portion of the muscle was divided to expose the cochlea bulla ventral to the facial nerve. The posterior semicircular canal (PSCC) was exposed dorsal to the cochlea bulla. A 0.5- to 1.0-mm-diameter otologic drill was used to make a small hole in the cochlea bulla, which was then widened sufficiently with forceps to visualize the stapedial artery and the RWM. A hole was also drilled in the PSCC with a 0.5-mm-diameter diamond drill; slow egress of perilymph confirmed a patent canalostomy. After waiting 5–10 min for perilymph egress to abate, 1.0 μL AAV vectors with 2.5% fast green dye (Sigma-Aldrich, St. Louis, MO, USA) was loaded into a borosilicate glass pipette (Harvard Apparatus, Hollison, MA, USA). For the dual-injection study, 0.5 μL of each AAV vector was loaded into the same glass pipette, creating 1:1 mixture of the dual vectors. Pipettes were manually controlled with a micropipette manipulator. The RWM was punctured gently in the center, and AAV was microinjected into the scala tympani for 5 min (30–40 nL per injection). Successful injections were confirmed by visualizing the efflux of green fluid from the PSCC canalostomy. After pulling out the pipette, the RWM niche was sealed quickly with a small plug of muscle to avoid leakage. The bony defect of the bulla and canal was sealed with small plugs of muscles and tissue adhesive. Total surgical time ranged from 30 to 50 min. When all procedures were finished, mice were placed on a heating pad for recovery with bedding. Pain was controlled with buprenorphine (0.05 mg/kg) and flunixin meglumine (2.5 mg/kg) for 3 days. Recovery was closely monitored daily for at least 5 days post-operatively.

Auditory Testing

ABRs were recorded as described previously.[4,34] All mice were anesthetized with an intra-peritoneal injection of ketamine (100 mg/kg) and xylazine (10 mg/kg). All recordings were conducted from both ears of all animals on a heating pad, and electrodes were placed subcutaneously in the vertex, underneath the left or right ear. Clicks were square pulses 100 ms in duration, and tone bursts were 3 ms in length

Figure 5. Transduction in the Stria Vascularis, Spiral Ganglion Cells, Saccules, and Scarpa's Ganglion Cells Is Vector Dependent

Midmodiolar cross-sectional images were immunostained with anti-GFP (green), anti-TuJ1 (red), phalloidin (magenta), and DAPI (blue). High-magnification views of the regions marked with white dotted squares in the cochlea show IHC, OHC, and SCs. Arrowheads indicate transduced cells in SV.

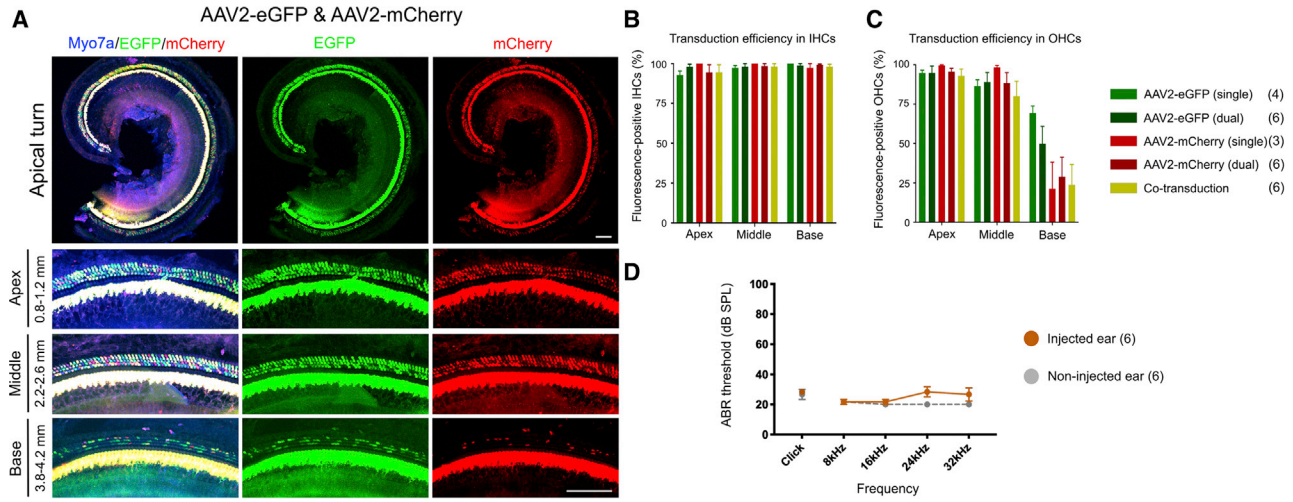

Figure 6. Dual-AAV2 and AAV2 Vectors Transduce Adult Murine IHCs and OHCs

(A) Cochleae harvested 2 weeks after co-administrating the combination of AAV2-2 via a RWM+CF approach in 4-week-old C3H/FeJ mice. Representative low-magnification images of whole-mount apical turns and high-magnification images of regions along the cochlea duct 0.8–1.2 mm (apex), 2.2–2.6 mm (middle), and 3.8–4.2 mm (base) from the apical tip. Cochleae were stained with Myo7a (blue) for labeling and imaged for native EGFP (green) and mCherry (red). Scale bar, 100 μm. (B and C) Quantitative comparison of IHC (B) and OHC (C) transduction efficiency assessed in 400-μm segments across different regions of the cochlea (apex, middle, and base) following the RWM+CF injection of the combinations of AAV2-2. (D) Click and tone-burst ABRs show auditory thresholds in injected (solid line) and non-injected (dashed line) ears were comparable following delivery of the combination of AAV2-2. Data are represented as mean ± SEM. Statistical analysis by Student's t test. *$p < 0.05$.

at distinct 8-, 16-, 24-, and 32-kHz frequencies. ABRs were measured with BioSigRZ (Tucker-Davis Technologies, Alachua, FL, USA) for both clicks and tone bursts, adjusting the stimulus levels in 5-dB increments between 10 and 90 dB sound pressure levels (SPLs) in both ears. Electrical signals were averaged over 512 repetitions. ABR threshold was defined as the lowest sound level at which a reproducible waveform could be observed. ABRs were measured 2 weeks after the injection. Responses from the right ear, which did not undergo surgery, were used as controls.

Immunohistochemistry

Bilateral inner ears were harvested 2 weeks after animals were sacrificed by CO_2 inhalation. Temporal bones were locally perfused and fixed in 4% paraformaldehyde for 2 h at room temperature, rinsed in PBS, and stored at 4°C in preparation for immunohistochemistry. Specimens were visualized with a dissection microscope and dissected for whole-mount analysis. In all of the cochlear and vestibular whole mounts, EGFP or mCherry was detected by its native fluorescence. Following infiltration using 0.3% Triton X-100 and blocking with 5% normal goat serum for 30 min at room temperature, tissues were incubated with rabbit polyclonal Myosin-VIIA antibody (#25–6790; Proteus Biosciences, Ramona, CA, USA) diluted 1:200 in PBS for 1 h. Subsequently, for the single-vector study, fluorescence-labeled goat anti-rabbit IgG Alexa Fluor 568 (#A-11036; Thermo Fisher Scientific, Rockford, IL, USA) in 1:500 dilution was used as a secondary antibody for 30 min. For the dual-vector study, goat anti-rabbit IgG Alexa Flour 405 (#A-31556; Thermo Fisher Scientific) in 1:500 dilution was used as a secondary antibody for 2 h. For cryo-sectioning, temporal bones were decalcified in 0.12 M EDTA for 2 days, cryoprotected in 15% and 30% sucrose, and embedded in OCT solution. Fourteen-micrometer-thick sections were prepared, and immunohistochemistry was performed. Following infiltration using 0.3% Triton X-100 and blocking with 5% normal goat serum for 30 min, the specimens were incubated in the following primary antibodies diluted in PBS: (1) mouse monoclonal anti-Green Fluorescent Protein antibody (MAB3580; Millipore Sigma, Burlington, MA, USA) at 1:200; and (2) rabbit polyclonal anti-Tubulin β-3 Antibody (#802001; BioLegend, San Diego, CA, USA) at 1:1,000 overnight at 4°C. We used goat anti-mouse IgG Alexa Fluor 488 (#A-11001; Thermo Fisher Scientific) and goat anti-rabbit IgG Alexa Fluor 568 (#A-11036; Thermo Fisher Scientific) diluted at 1:500 in PBS as secondary antibodies for 30 min. Filamentous actin was labeled by a 30-min incubation of phalloidin conjugated to Alexa Fluor 647 (#A22287; Thermo Fisher Scientific) in 1:100 dilution. Specimens were mounted with ProLong Diamond Antifade Mountant with DAPI (#P36962; Thermo Fisher Scientific) for the single-vector study and ProLong Diamond Antifade Mountant (#P36961; Thermo Fisher Scientific) for the dual-vector study, and observed with a Leica TCS SP8 confocal microscope (Leica Microsystems, Bannockburn, IL, USA).

Cell Counts and Transduction Efficiency Analysis

Cell counts and transduction efficiency analysis were performed as described previously.[4,35] z stack images of whole mounts were collected at 10–20× on a Leica SP8 confocal microscope. Each turn of the cochlea was analyzed: 0.8–1.2 mm (apex), 2.2–2.6 mm (middle), and 3.8–4.2 mm (base) of the total length from the apical tip.

The corresponding approximate frequencies are 8, 16, and 32 kHz, respectively.[36] Maximum intensity projections of z stacks were generated for each field of view, and images were prepared using LAS X (Leica Microsystems) to meet equal conditions. IHCs with positive EGFP and overlapping Myo7a were counted per 400-μm cochlear sections for each turn in each specimen with ImageJ Cell Counter (NIH Image). The total number of HCs and GFP-positive HCs were summed and converted to a percentage.

Statistical Analysis

Sample sizes are noted in the figure legends. Cell counting and ABR data are presented as mean ± SEM. Statistical analysis was performed using Prism 8 software package (GraphPad, San Diego, CA, USA). Two groups were compared using unpaired two-tailed Student's t test. For comparisons of more than two groups, one-way ANOVA was performed and followed by *post hoc* test with Bonferroni correction of pairwise group differences. $p < 0.05$ was considered statistically significant.

SUPPLEMENTAL INFORMATION

Supplemental Information can be found online at https://doi.org/10.1016/j.omtm.2020.05.007.

AUTHOR CONTRIBUTIONS

Conceptualization, H.Y., R.O., S.B.S., and R.J.H.S.; Methodology, R.O., H.Y., S.B.S., and R.J.H.S.; Investigation, R.O. and H.Y.; Writing – Original Draft, R.O., H.Y., and S.B.S.; Writing – Review & Editing, R.O., H.Y., S.B.S., and R.J.H.S.; Funding Acquisition, R.J.H.S. and S.B.S.; Resources, L.H.V. and R.J.H.S.; Supervision, R.J.H.S.

CONFLICTS OF INTEREST

L.H.V. is co-inventor on patents covering AAV9 and Anc80 and their use in the inner ear. L.H.V. is co-founder and SAB member to Akouos, a hearing gene therapy company, and a founder, consultant, and board member of TDTx, a company developing AAV gene therapies. He also consults for various biopharma companies in the gene therapy space. These interests were reviewed and are managed by MEE and Partners HealthCare in accordance with their conflict of interest policies. R.J.H.S. is co-founder and SAB member to Akouos.

ACKNOWLEDGMENTS

This study was supported by NIH/NIDCD grants T32 DC000040–17 (to S.B.S.) and R01 DC017955 (to R.J.H.S.), and AAO-HNSF Resident Research Grant 2013 (to S.B.S.).

REFERENCES

1. Ahmed, H., Shubina-Oleinik, O., and Holt, J.R. (2017). Emerging gene therapies for genetic hearing loss. J. Assoc. Res. Otolaryngol. *18*, 649–670.
2. Xia, L., and Yin, S. (2013). Local gene transfection in the cochlea (Review). Mol. Med. Rep. *8*, 3–10.
3. Pillay, S., Zou, W., Cheng, F., Puschnik, A.S., Meyer, N.L., Ganaie, S.S., Deng, X., Wosen, J.E., Davulcu, O., Yan, Z., et al. (2017). Adeno-associated Virus (AAV) serotypes have distinctive interactions with domains of the cellular AAV receptor. J. Virol. *91*, e00391-17.
4. Yoshimura, H., Shibata, S.B., Ranum, P.T., and Smith, R.J.H. (2018). Enhanced viral-mediated cochlear gene delivery in adult mice by combining canal fenestration with round window membrane inoculation. Sci. Rep. *8*, 2980.
5. Pan, B., Askew, C., Galvin, A., Heman-Ackah, S., Asai, Y., Indzhykulian, A.A., Jodelka, F.M., Hastings, M.L., Lentz, J.J., Vandenberghe, L.H., et al. (2017). Gene therapy restores auditory and vestibular function in a mouse model of Usher syndrome type 1c. Nat. Biotechnol. *35*, 264–272.
6. Askew, C., Rochat, C., Pan, B., Asai, Y., Ahmed, H., Child, E., Schneider, B.L., Aebischer, P., and Holt, J.R. (2015). Tmc gene therapy restores auditory function in deaf mice. Sci. Transl. Med. *7*, 295ra108.
7. Landegger, L.D., Pan, B., Askew, C., Wassmer, S.J., Gluck, S.D., Galvin, A., Taylor, R., Forge, A., Stankovic, K.M., Holt, J.R., and Vandenberghe, L.H. (2017). A synthetic AAV vector enables safe and efficient gene transfer to the mammalian inner ear. Nat. Biotechnol. *35*, 280–284.
8. Tao, Y., Huang, M., Shu, Y., Ruprecht, A., Wang, H., Tang, Y., Vandenberghe, L.H., Wang, Q., Gao, G., Kong, W.J., and Chen, Z.Y. (2018). Delivery of Adeno-Associated Virus Vectors in Adult Mammalian Inner-Ear Cell Subtypes Without Auditory Dysfunction. Hum. Gene Ther. *29*, 492–506.
9. Kilpatrick, L.A., Li, Q., Yang, J., Goddard, J.C., Fekete, D.M., and Lang, H. (2011). Adeno-associated virus-mediated gene delivery into the scala media of the normal and deafened adult mouse ear. Gene Ther. *18*, 569–578.
10. Shu, Y., Tao, Y., Wang, Z., Tang, Y., Li, H., Dai, P., Gao, G., and Chen, Z.Y. (2016). Identification of Adeno-Associated Viral Vectors That Target Neonatal and Adult Mammalian Inner Ear Cell Subtypes. Hum. Gene Ther. *27*, 687–699.
11. Omichi, R., Shibata, S.B., Morton, C.C., and Smith, R.J.H. (2019). Gene therapy for hearing loss. Hum. Mol. Genet. *28* (R1), R65–R79.
12. Colella, P., Ronzitti, G., and Mingozzi, F. (2017). Emerging Issues in AAV-Mediated *In Vivo* Gene Therapy. Mol. Ther. Methods Clin. Dev. *8*, 87–104.
13. Akil, O., Dyka, F., Calvet, C., Emptoz, A., Lahlou, G., Nouaille, S., Boutet de Monvel, J., Hardelin, J.P., Hauswirth, W.W., Avan, P., et al. (2019). Dual AAV-mediated gene therapy restores hearing in a DFNB9 mouse model. Proc. Natl. Acad. Sci. USA *116*, 4496–4501.
14. Al-Moyed, H., Cepeda, A.P., Jung, S., Moser, T., Kügler, S., and Reisinger, E. (2019). A dual-AAV approach restores fast exocytosis and partially rescues auditory function in deaf otoferlin knock-out mice. EMBO Mol. Med. *11*, e9396.
15. Maddalena, A., Dell'Aquila, F., Giovannelli, P., Tiberi, P., Wanderlingh, L.G., Montefusco, S., Tornabene, P., Iodice, C., Visconte, F., Carissimo, A., et al. (2018). High-Throughput Screening Identifies Kinase Inhibitors That Increase Dual Adeno-Associated Viral Vector Transduction In Vitro and in Mouse Retina. Hum. Gene Ther. *29*, 886–901.
16. Suzuki, J., Hashimoto, K., Xiao, R., Vandenberghe, L.H., and Liberman, M.C. (2017). Cochlear gene therapy with ancestral AAV in adult mice: complete transduction of inner hair cells without cochlear dysfunction. Sci. Rep. *7*, 45524.
17. Nass, S.A., Mattingly, M.A., Woodcock, D.A., Burnham, B.L., Ardinger, J.A., Osmond, S.E., Frederick, A.M., Scaria, A., Cheng, S.H., and O'Riordan, C.R. (2017). Universal Method for the Purification of Recombinant AAV Vectors of Differing Serotypes. Mol. Ther. Methods Clin. Dev. *9*, 33–46.
18. Gu, X., Chai, R., Guo, L., Dong, B., Li, W., Shu, Y., Huang, X., and Li, H. (2019). Transduction of Adeno-Associated Virus Vectors Targeting Hair Cells and Supporting Cells in the Neonatal Mouse Cochlea. Front. Cell. Neurosci. *13*, 8.
19. Tan, F., Chu, C., Qi, J., Li, W., You, D., Li, K., Chen, X., Zhao, W., Cheng, C., Liu, X., et al. (2019). AAV-ie enables safe and efficient gene transfer to inner ear cells. Nat. Commun. *10*, 3733.
20. Isgrig, K., McDougald, D.S., Zhu, J., Wang, H.J., Bennett, J., and Chien, W.W. (2019). AAV2.7m8 is a powerful viral vector for inner ear gene therapy. Nat. Commun. *10*, 427.
21. Shibata, S.B., Di Pasquale, G., Cortez, S.R., Chiorini, J.A., and Raphael, Y. (2009). Gene transfer using bovine adeno-associated virus in the guinea pig cochlea. Gene Ther. *16*, 990–997.
22. Hordeaux, J., Wang, Q., Katz, N., Buza, E.L., Bell, P., and Wilson, J.M. (2018). The Neurotropic Properties of AAV-PHP.B Are Limited to C57BL/6J Mice. Mol. Ther. *26*, 664–668.

23. Hordeaux, J., Yuan, Y., Clark, P.M., Wang, Q., Martino, R.A., Sims, J.J., Bell, P., Raymond, A., Stanford, W.L., and Wilson, J.M. (2019). The GPI-Linked Protein LY6A Drives AAV-PHP.B Transport across the Blood-Brain Barrier. Mol. Ther. *27*, 912–921.

24. Dong, J.Y., Fan, P.D., and Frizzell, R.A. (1996). Quantitative analysis of the packaging capacity of recombinant adeno-associated virus. Hum. Gene Ther. *7*, 2101–2112.

25. Duan, D., Yue, Y., and Engelhardt, J.F. (2001). Expanding AAV packaging capacity with trans-splicing or overlapping vectors: a quantitative comparison. Mol. Ther. *4*, 383–391.

26. Yan, Z., Zhang, Y., Duan, D., and Engelhardt, J.F. (2000). Trans-splicing vectors expand the utility of adeno-associated virus for gene therapy. Proc. Natl. Acad. Sci. USA *97*, 6716–6721.

27. Lai, Y., Yue, Y., Liu, M., Ghosh, A., Engelhardt, J.F., Chamberlain, J.S., and Duan, D. (2005). Efficient in vivo gene expression by trans-splicing adeno-associated viral vectors. Nat. Biotechnol. *23*, 1435–1439.

28. Reich, S.J., Auricchio, A., Hildinger, M., Glover, E., Maguire, A.M., Wilson, J.M., and Bennett, J. (2003). Efficient trans-splicing in the retina expands the utility of adeno-associated virus as a vector for gene therapy. Hum. Gene Ther. *14*, 37–44.

29. Trapani, I., Colella, P., Sommella, A., Iodice, C., Cesi, G., de Simone, S., Marrocco, E., Rossi, S., Giunti, M., Palfi, A., et al. (2014). Effective delivery of large genes to the retina by dual AAV vectors. EMBO Mol. Med. *6*, 194–211.

30. Tornabene, P., Trapani, I., Minopoli, R., Centrulo, M., Lupo, M., de Simone, S., Tiberi, P., Dell'Aquila, F., Marrocco, E., Iodice, C., et al. (2019). Intein-mediated protein trans-splicing expands adeno-associated virus transfer capacity in the retina. Sci. Transl. Med. *11*, eaav4523.

31. Carvalho, L.S., Turunen, H.T., Wassmer, S.J., Luna-Velez, M.V., Xiao, R., Bennett, J., and Vandenberghe, L.H. (2017). Evaluating Efficiencies of Dual AAV Approaches for Retinal Targeting. Front. Neurosci. *11*, 503.

32. Colella, P., Trapani, I., Cesi, G., Sommella, A., Manfredi, A., Puppo, A., Iodice, C., Rossi, S., Simonelli, F., Giunti, M., et al. (2014). Efficient gene delivery to the cone-enriched pig retina by dual AAV vectors. Gene Ther. *21*, 450–456.

33. Sanmiguel, J., Gao, G., and Vandenberghe, L.H. (2019). Quantitative and Digital Droplet-Based AAV Genome Titration. Methods Mol. Biol. *1950*, 51–83.

34. Yoshimura, H., Shibata, S.B., Ranum, P.T., Moteki, H., and Smith, R.J.H. (2019). Targeted Allele Suppression Prevents Progressive Hearing Loss in the Mature Murine Model of Human TMC1 Deafness. Mol. Ther. *27*, 681–690.

35. Shibata, S.B., Yoshimura, H., Ranum, P.T., Goodwin, A.T., and Smith, R.J.H. (2017). Intravenous rAAV2/9 injection for murine cochlear gene delivery. Sci. Rep. *7*, 9609.

36. Viberg, A., and Canlon, B. (2004). The guide to plotting a cochleogram. Hear. Res. *197*, 1–10.